Subproblem Approach for Thin Shell Dual Finite Element Formulations

Vuong Q. Dang[1], Patrick Dular[1,2], Ruth V. Sabariego[1], Laurent Krähenbühl[3], and Christophe Geuzaine[1]

[1]University of Liège, Dept. of Electrical Engineering and Computer Science, ACE, B-4000 Liège, Belgium
[2]Fonds de la Recherche Scientifique-F.R.S.-FNRS, B-1000 Brussels, Belgium
[3]Université de Lyon, Ampère (CNRS UMR5005), École Centrale de Lyon, F-69134 Écully Cedex, France

A subproblem technique is applied to dual thin shell finite element formulations. Both the magnetic vector potential and magnetic field formulations are considered. The subproblem approach developed herein couples three problems: a simplified model with only inductors, a thin region problem using approximate interface conditions and a correction problem to improve the accuracy of the thin shell approximation, in particular near their edges and corners. Each problem has its own geometry and is solved on its associated finite element mesh.

***Index Terms*—Eddy current, finite element method (FEM), magnetodynamics, subproblem method (SPM), thin shell (TS).**

I. Introduction

THE solution by means of the subproblem method (SPM) provides advantages in repetitive analyses and also helps improving the overall accuracy of the solution [1], [2]. The SPM allows to benefit from previous computations instead of starting a new complete finite element (FE) solution for any variation of geometrical or physical characteristics. Furthermore, each subproblem (SP) has its own separate mesh, which increases computational efficiency.

The SPM for dual FE $\boldsymbol{b}$- and $\boldsymbol{h}$-formulations are herein developed within the thin shell (TS) framework [1], [3], [4], pointing out their complementarity. A first problem (SP 1) involving only massive or stranded inductors is solved on a simplified mesh without thin regions. Its solution gives surface sources (SSs) for a second problem with TS (SP 2) through interface conditions (ICs) based on 1-D approximations [3], [4]. The TS solution is then corrected in a third problem (SP 3) via SSs and volume sources (VSs), that suppress the TS representation and add the actual volume. This corrects the field distribution near edges and corners, where the TS model inaccuracies occur. The method is validated on test problems by comparison with classical FE solutions.

II. Definition of the Subproblem Approach

A. Canonical Magnetodynamic or Static Problem

A canonical magnetodynamic or static problem p, to be solved at step p of the SPM, is defined in a domain Ω_p, with boundary $\partial\Omega_p = \Gamma_p = \Gamma_{h,p} \cup \Gamma_{b,p}$. The eddy current conducting part of Ω_p is denoted $\Omega_{c,p}$ and the non-conducting region $\Omega_{c,p}^C$, with $\Omega_p = \Omega_{c,p} \cup \Omega_{c,p}^C$. Stranded inductors belong to $\Omega_{c,p}^C$, whereas massive inductors belong to $\Omega_{c,p}$. The governing equations, material relations and boundary conditions (BCs) of SPs $p = 1$, 2 and 3 are

$$\operatorname{curl} \boldsymbol{h}_p = \boldsymbol{j}_p, \quad \operatorname{div} \boldsymbol{b}_p = 0, \quad \operatorname{curl} \boldsymbol{e}_p = -\partial_t \boldsymbol{b}_p \quad \text{(1a-b-c)}$$

$$\boldsymbol{h}_p = \mu_p^{-1}\boldsymbol{b}_p + \boldsymbol{h}_{s,p}, \quad \boldsymbol{b}_p = \mu_p \boldsymbol{h}_p + \boldsymbol{b}_{s,p} \quad \text{(2a-b)}$$

$$\boldsymbol{j}_p = \sigma_p \boldsymbol{e}_p + \boldsymbol{j}_{s,p}, \quad \boldsymbol{e}_p = \sigma_p^{-1}\boldsymbol{j}_p + \boldsymbol{e}_{s,p} \quad \text{(3a-b)}$$

$$\boldsymbol{n} \times \boldsymbol{h}_p|_{\Gamma_{h,p}} = \boldsymbol{j}_{su,p}, \quad \boldsymbol{n} \cdot \boldsymbol{b}_p|_{\Gamma_{b,p}} = \boldsymbol{b}_{su,p} \quad \text{(4a-b)}$$

$$\boldsymbol{n} \times \boldsymbol{e}_p|_{\Gamma_{e,p} \subset \Gamma_{b,p}} = \boldsymbol{k}_{su,p} \quad \text{(4c)}$$

where $\boldsymbol{h}_p$ is the magnetic field, $\boldsymbol{b}_p$ is the magnetic flux density, $\boldsymbol{e}_p$ is the electric field, $\boldsymbol{j}_{s,p}$ is the electric current density, μ_p is the magnetic permeability, σ_p is the electric conductivity and $\boldsymbol{n}$ is the unit normal exterior to Ω_p.

The fields $\boldsymbol{h}_{s,p}, \boldsymbol{b}_{s,p}, \boldsymbol{j}_{s,p}$ and $\boldsymbol{e}_{s,p}$ in (2a), (2b) and (3a), (3b) are VSs that can be used to account for changes of permeability or conductivity in each SP [2]. The fields $\boldsymbol{j}_{su,p}, \boldsymbol{b}_{su,p}$ and $\boldsymbol{k}_{su,p}$ in (4a-b-c) are SSs and generally equal zero for classical homogeneous BCs. ICs can define their discontinuities through any interface γ_p (with sides γ_p^+ and γ_p^-) in Ω_p, with the notation $[\cdot]_{\gamma_p} = |_{\gamma_p^+} - |_{\gamma_p^-}$. ICs equal zero for common continuous field traces. If nonzero, they define possible SSs that account for particular phenomena occuring in the idealized thin regions between γ_p^+ and γ_p^- [5], [7]. A typical case appears when some field traces in a previous problem are forced to be discontinuous, whereas their continuity must be recovered via a correction problem p; with the SSs fixed as the opposite of the trace solution of previous SP.

B. From Inductor Alone to TS

The TS model [4] is defined in SP 2 following the already calculated inductor source field from SP 1. Its SSs are defined via the BCs and ICs of impedance-type boundary conditions (IBC) combined with contributions from SP 1. The $\boldsymbol{b}$-formulation uses a magnetic vector potential $\boldsymbol{a}$ (such that curl $\boldsymbol{a} = \boldsymbol{b}$), split as $\boldsymbol{a} = \boldsymbol{a}_c + \boldsymbol{a}_d$ [4]. An analogous decomposition is done for the $\boldsymbol{h}$-formulation, with $\boldsymbol{h} = \boldsymbol{h}_c + \boldsymbol{h}_d$. The fields $\boldsymbol{a}_c$, $\boldsymbol{h}_c$ and $\boldsymbol{a}_d$, $\boldsymbol{h}_d$ are continuous and discontinuous respectively through the TS.

1) SSs for $\boldsymbol{b}$-Formulation: Even if there is no thin region in SP 1, we have to foresee its future addition and allow for the coupling of relative constraint between SP 1 and SP 2 via the corresponding ICs with $\gamma_p = \gamma_p^{\pm} = \gamma_1^{\pm} = \gamma_2^{\pm}$ and $\boldsymbol{n}_p = -\boldsymbol{n}$ for the TS. One has for SPs 1 and 2 [4]

$$[\boldsymbol{n}\times\boldsymbol{h}_1]_{\gamma_1} = \boldsymbol{n}\times\boldsymbol{h}_1|_{\gamma_1^+} - \boldsymbol{n}\times\boldsymbol{h}_1|_{\gamma_1^-} = 0 \quad (5)$$

$$[\boldsymbol{n}\times\boldsymbol{h}]_{\gamma_2} = [\boldsymbol{n}\times\boldsymbol{h}_1]_{\gamma_2} + [\boldsymbol{n}\times\boldsymbol{h}_2]_{\gamma_2} = \sigma\beta\partial_t(2\boldsymbol{a}_c + \boldsymbol{a}_d) \quad (6)$$

$$\boldsymbol{n}\times\boldsymbol{h}_1|_{\gamma_{2+}} + \boldsymbol{n}\times\boldsymbol{h}_2|_{\gamma_{2+}} = \frac{1}{2}\left[\sigma\beta\partial_t(2\boldsymbol{a}_c + \boldsymbol{a}_d) + \frac{1}{\mu\beta}\boldsymbol{a}_d\right] \quad (7)$$

Manuscript received July 05, 2011; revised October 12, 2011; accepted November 08, 2011. Corresponding
author: V. Q. Dang (e-mail: quocvuong.dang@ulg.ac.be).

$$\beta = \gamma_p^{-1} \tanh\left(\frac{d_p\gamma_p}{2}\right), \gamma_p = \frac{1+j}{\delta_p}, \delta_p = \sqrt{2/\omega\sigma_p\mu_p} \qquad (8)$$

where d_p is the TS thickness, δ_p is the skin depth, $\omega = 2\pi f$, j is the imaginary unit. For $\delta_p \gg d_p$, one has $\beta \approx d_p/2$. In statics, (6) is equal to zero. The discontinuity $[\boldsymbol{n} \times \boldsymbol{h}_1]_{\gamma_2}$ in (6) is actually zero, with no TS in SP 1, i.e. $[\boldsymbol{n} \times \boldsymbol{h}_1]_{\gamma_1} = [\boldsymbol{n} \times \boldsymbol{h}_1]_{\gamma_2} = 0$.

2) SSs for $\boldsymbol{h}$-Formulation: One gets for SPs 1 and 2 [4]

$$[\boldsymbol{n}\times\boldsymbol{e}_1]_{\gamma_1} = \boldsymbol{n}\times\boldsymbol{e}_1|_{\gamma_1^+} - \boldsymbol{n}\times\boldsymbol{e}_1|_{\gamma_1^-} = 0 \qquad (9)$$

$$[\boldsymbol{n}\times\boldsymbol{e}]_{\gamma_2} = [\boldsymbol{n}\times\boldsymbol{e}_1]_{\gamma_2} + [\boldsymbol{n}\times\boldsymbol{e}_2]_{\gamma_2} = \sigma\beta\partial_t(2\boldsymbol{h}_c + \boldsymbol{h}_d) \qquad (10)$$

$$\boldsymbol{n}\times\boldsymbol{e}_1|_{\gamma_2+} + \boldsymbol{n}\times\boldsymbol{e}_2|_{\gamma_2+} = \frac{1}{2}\left[\sigma\beta\partial_t(2\boldsymbol{h}_c + \boldsymbol{h}_d) + \frac{1}{\mu\beta}\boldsymbol{h}_d\right]. \qquad (11)$$

In statics, (10) is equal to zero. Because there is no TS in SP 1, $[\boldsymbol{n} \times \boldsymbol{e}_1]_{\gamma_1} = [\boldsymbol{n} \times \boldsymbol{e}_1]_{\gamma_2} = 0$ in (10).

C. From TS to Volume Model

The TS solution in SP 2 is next corrected by SP 3 that overcomes the TS assumptions [4]. To correct the TS model, one has to suppress the TS representation via SSs opposed to TS ICs, and to add the actual volume shell via VSs that account for volume changes of μ_p and σ_p from the properties of ambient region in SP 2 to these of volume shell in SP 3 (with $\mu_2 = \mu_0$, $\mu_3 = \mu_{volume}$, $\sigma_2 = 0$ and $\sigma_3 = \sigma_{volume}$). This correction can be limited to the neighborhood of the shell, which allows to benefit from a reduction of the extension of the associated mesh [1]. The VSs for SP 3 are thus [1], [7]

$$\boldsymbol{h}_{s,3} = \left(\mu_3^{-1} - \mu_2^{-1}\right)\boldsymbol{b}_2, \quad \boldsymbol{b}_{s,3} = (\mu_3 - \mu_2)\boldsymbol{h}_2 \qquad (12a\text{-}b)$$

$$\boldsymbol{j}_{s,3} = (\sigma_3 - \sigma_2)\boldsymbol{e}_2, \quad \boldsymbol{e}_{s,3} = \left(\sigma_3^{-1} - \sigma_2^{-1}\right)\boldsymbol{j}_2. \qquad (13a\text{-}b)$$

III. Finite Element Weak Formulations

A. Magnetic Vector Potential Formulation

The weak $\boldsymbol{b}_p$-formulation (in terms of $\boldsymbol{a}_p$) is obtained from the weak form of Ampère's law (1a), i.e. [1]–[5]. For SPs 1 and 2, they read

$$\begin{aligned}&\left(\mu_1^{-1}\mathrm{curl}\,\boldsymbol{a}_1, \mathrm{curl}\,\boldsymbol{a}'_1\right)_{\Omega_1} + \langle\boldsymbol{n}\times\boldsymbol{h}_1, \boldsymbol{a}'_1\rangle_{\Gamma_{h,1}} + \langle\boldsymbol{n}\times\boldsymbol{h}_1, \boldsymbol{a}'_1\rangle_{\Gamma_{b,1}}\\ &+ \langle[\boldsymbol{n}\times\boldsymbol{h}_1]_{\gamma_1}, \boldsymbol{a}'_1\rangle_{\gamma_1} = \left(\boldsymbol{j}_{s,1}, \boldsymbol{a}'_1\right)_{\Omega_1}, \quad \forall\boldsymbol{a}'_1 \in F_1^1(\Omega_1) \qquad (14)\end{aligned}$$

$$\begin{aligned}&\left(\mu_2^{-1}\mathrm{curl}\,\boldsymbol{a}_2, \mathrm{curl}\,\boldsymbol{a}'_2\right)_{\Omega_2} + (\sigma_2\partial_t\boldsymbol{a}_2, \boldsymbol{a}'_2)_{\Omega_2}\\ &+ (\sigma_2 \mathrm{grad}\, v_2, \boldsymbol{a}'_2)_{\Omega_2} + \langle\boldsymbol{n}\times\boldsymbol{h}_2, \boldsymbol{a}'_2\rangle_{\Gamma_{h,2}} + \langle\boldsymbol{n}\times\boldsymbol{h}_2, \boldsymbol{a}'_2\rangle_{\Gamma_{b,2}}\\ &+ \langle[\boldsymbol{n}\times\boldsymbol{h}_2]_{\gamma_2}, \boldsymbol{a}'_2\rangle_{\gamma_2} = 0, \quad \forall\boldsymbol{a}'_2 \in F_2^1(\Omega_2) \qquad (15)\end{aligned}$$

where $F_p^1(\Omega_p)$ is a curl-conform function space defined on Ω_p, gauged in $\Omega_{c,p}^C$, and containing the basis functions for $\boldsymbol{a}_p$ as well as for the test function $\boldsymbol{a}'_p$ (at the discrete level, this space is defined by edge FEs; the gauge is based on the tree-cotree technique); $(\cdot,\cdot)_\Omega$ and $\langle\cdot,\cdot\rangle_\Gamma$ denote a volume integral in Ω and a surface integral on Γ, respectively, of the product of their vector field arguments. The surface integral terms on $\Gamma_{h,p}$ account for natural BCs of type (4a), usually zero. Note that the unknown term on the surface $\Gamma_{b,p}$ with essential BCs on $\boldsymbol{n}.\boldsymbol{b}_p$ is often omitted because it does not locally contribute to (14). It will be used for post-processing a solution, a part of which, $\boldsymbol{n}\times\boldsymbol{h}_p|_{\Gamma_{b,p}}$, acts as a SS in further problems [5], [7].

The term $\langle[\boldsymbol{n} \times \boldsymbol{h}_2]_{\gamma_2}, \boldsymbol{a}'_2\rangle$ in (15) can be rewritten as

$$\begin{aligned}\langle[\boldsymbol{n}\times\boldsymbol{h}_2]_{\gamma_2}, \boldsymbol{a}'_2\rangle_{\gamma_2} &= \langle[\boldsymbol{n}\times\boldsymbol{h}_2]_{\gamma_2}, \boldsymbol{a}'_c + \boldsymbol{a}'_d\rangle_{\gamma_2}\\ &= \langle[\boldsymbol{n}\times\boldsymbol{h}_2]_{\gamma_2}, \boldsymbol{a}'_c\rangle_{\gamma_2} + \langle[\boldsymbol{n}\times\boldsymbol{h}_2]_{\gamma_2}, \boldsymbol{a}'_d\rangle_{\gamma_2} \qquad (16)\end{aligned}$$

splitting test function $\boldsymbol{a}'_2$ into the continuous and discontinuous parts $\boldsymbol{a}'_c$ and $\boldsymbol{a}'_d$, with $\boldsymbol{a}'_d$ null on the TS side γ_2^- [4]. This gives

$$\langle[\boldsymbol{n} \times \boldsymbol{h}_2]_{\gamma_2}, \boldsymbol{a}'_2\rangle_{\gamma_2} = \langle[\boldsymbol{n} \times \boldsymbol{h}_2]_{\gamma_2}, \boldsymbol{a}'_c\rangle_{\gamma_2} + \langle\boldsymbol{n} \times \boldsymbol{h}_2, \boldsymbol{a}'_d\rangle_{\gamma_2^+}. \qquad (17)$$

The $\boldsymbol{h}_p$ trace discontinuity $\langle[\boldsymbol{n} \times \boldsymbol{h}_2]_{\gamma_2}, \boldsymbol{a}'_c\rangle_{\gamma_2}$ in (17) is given by (6), i.e.

$$\langle[\boldsymbol{n}\times\boldsymbol{h}_2]_{\gamma_2}, \boldsymbol{a}'_c\rangle_{\gamma_2} = \langle[\boldsymbol{n}\times\boldsymbol{h}]_{\gamma_2}, \boldsymbol{a}'_c\rangle_{\gamma_2} = \langle\sigma\beta\partial_t(2\boldsymbol{a}_c + \boldsymbol{a}_d), \boldsymbol{a}'_c\rangle_{\gamma_2}. \qquad (18)$$

The term $\langle\boldsymbol{n} \times \boldsymbol{h}_2, \boldsymbol{a}'_d\rangle_{\gamma_2^+}$ in (17) related to the positive side of the TS is given by (7), suppressing $\boldsymbol{n}\times\boldsymbol{h}_1|_{\gamma_2^+}$ of SP 1 and adding the actual TS BC. For that, the term $\langle\boldsymbol{n} \times \boldsymbol{h}_1, \boldsymbol{a}'_d\rangle_{\gamma_2^+}$ is a SS that can be naturally expressed via the weak formulation of SP 1 in (14), i.e.

$$-\langle\boldsymbol{n} \times \boldsymbol{h}_1, \boldsymbol{a}'_d\rangle_{\gamma_2^+} = \left(\mu_1^{-1}\mathrm{curl}\,\boldsymbol{a}_1, \mathrm{curl}\,\boldsymbol{a}'_d\right)_{\Omega_2 = \Omega_1}. \qquad (19)$$

The contribution of the volume integral in (19) is limited to a single layer of FEs on the positive side of $\Omega_2^+ = \Omega_1^+$ touching $\gamma_2^+ = \gamma_1^+$, because it involves only the trace $\boldsymbol{n} \times \boldsymbol{a}'_d|_{\gamma_2^+}$. At the discrete level, the source $\boldsymbol{a}_1$, initially in mesh of SP 1, has to be projected in mesh of SP 2 [1], [10]. The TS SP 2 solution of (15) is then corrected by SP 3 via the VSs (12a) and (13a). Fields have also to be transferred from the mesh of TS SP 2 to the mesh of SP 3. From that, the weak form for SP 3 is

$$\begin{aligned}&\left(\mu_3^{-1}\mathrm{curl}\,\boldsymbol{a}_3, \mathrm{curl}\,\boldsymbol{a}'_3\right)_{\Omega_3} + (\sigma_3\partial_t\boldsymbol{a}_3, \boldsymbol{a}'_3)_{\Omega_{c3}} + \langle\boldsymbol{n}\times\boldsymbol{h}_3, \boldsymbol{a}'_3\rangle_{\Gamma_{h,3}}\\ &+ \langle\boldsymbol{n}\times\boldsymbol{h}_3, \boldsymbol{a}'_3\rangle_{\Gamma_{b,3}} + (\sigma_3 \text{ grad } v_3, \boldsymbol{a}'_3)_{\Omega_{c3}} + (\boldsymbol{h}_{s,3}, \mathrm{curl}\,\boldsymbol{a}'_3)_{\Omega_3}\\ &+ \left(\boldsymbol{j}_{s,3}, \boldsymbol{a}'_3\right)_{\Omega_{c3}} = 0, \quad \forall\boldsymbol{a}'_3 \in F_3^1(\Omega_3). \qquad (20)\end{aligned}$$

B. Magnetic Field Formulation

The weak $\boldsymbol{h}_p$-formulation is obtained from the weak form of Faraday's law (1c) [1], [7]. The field $\boldsymbol{h}_p$ is split into two parts, $\boldsymbol{h}_p = \boldsymbol{h}_{s,p} + \boldsymbol{h}_{r,p}$, where $\boldsymbol{h}_{s,p}$ is a source field defined by curl $\boldsymbol{h}_{s,p} = \boldsymbol{j}_{s,p}$, and $\boldsymbol{h}_{r,p}$ is unknown. For SPs 1 and 2, one has

$$\begin{aligned}&\partial_t\left(\mu_1\boldsymbol{h}_1, \boldsymbol{h}'_1\right)_{\Omega_1} + \partial_t\left(\mu_1\boldsymbol{h}_{s1}, \boldsymbol{h}'_1\right)_{\Omega_1} + \left\langle\boldsymbol{n}\times\boldsymbol{e}_1, \boldsymbol{h}'_1\right\rangle_{\Gamma_{e,1}}\\ &+ \left\langle[\boldsymbol{n}\times\boldsymbol{e}_1]_{\gamma_1}, \boldsymbol{h}'_1\right\rangle_{\gamma_1} = 0, \ \forall\boldsymbol{h}'_1 \in F_1^1(\Omega_1) \qquad (21)\end{aligned}$$

$$\begin{aligned}&\partial_t\left(\mu_2\boldsymbol{h}_2, \boldsymbol{h}'_2\right)_{\Omega_2} + \left(\sigma_2^{-1}\mathrm{curl}\,\boldsymbol{h}_2, \mathrm{curl}\,\boldsymbol{h}'_2\right)_{\Omega_2} + \left\langle\boldsymbol{n}\times\boldsymbol{e}_2, \boldsymbol{h}'_2\right\rangle_{\Gamma_{e,2}}\\ &+ \left\langle[\boldsymbol{n}\times\boldsymbol{e}_2]_{\gamma_2}, \boldsymbol{h}'_c\right\rangle_{\gamma_2} = 0, \ \forall\boldsymbol{h}'_2 \in F_2^1(\Omega_2) \qquad (22)\end{aligned}$$

where $F_p^1(\Omega_p)$ is a curl-conform function space defined on Ω_p and containing the basis functions for $\boldsymbol{h}$ as well as for the test function $\boldsymbol{h}'$. The surface integral terms on $\Gamma_{e,p}$ account for natural BCs of type (4c), usually zero.

The term $\left\langle[\boldsymbol{n} \times \boldsymbol{e}_2]_{\gamma_2}, \boldsymbol{h}'_2\right\rangle_{\gamma_2}$ in (22) expresses as

$$\begin{aligned}\left\langle[\boldsymbol{n}\times\boldsymbol{e}_2]_{\gamma_2}, \boldsymbol{h}'_2\right\rangle_{\gamma_2} &= \left\langle[\boldsymbol{n}\times\boldsymbol{e}_2]_{\gamma_2}, \boldsymbol{h}'_c + \boldsymbol{h}'_d\right\rangle_{\gamma_2}\\ &= \left\langle[\boldsymbol{n}\times\boldsymbol{e}_2]_{\gamma_2}, \boldsymbol{h}'_c\right\rangle_{\gamma_2} + \left\langle[\boldsymbol{n}\times\boldsymbol{e}_2]_{\gamma_2}, \boldsymbol{h}'_d\right\rangle_{\gamma_2} \qquad (23)\end{aligned}$$

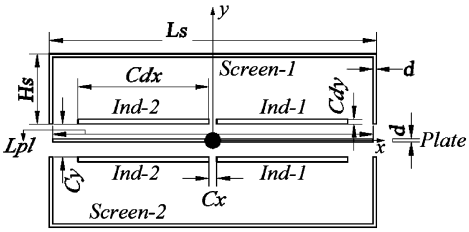

Fig. 1. Shielded induction heater ($d = 2 \div 6$ mm, $L_{pl} = 2$ m, $L_s = 2$ m + 2 d, $H_s = 0.4$ m, $C_{dx} = 0.8$ m, $C_{dy} = 0.01$ m, $C_y = 0.2$ m, $C_x = 0.05$ m).

splitting test function $\boldsymbol{h}_2'$ into continuous and discontinuous parts $\boldsymbol{h}_c'$ and $\boldsymbol{h}_d'$, with $\boldsymbol{h}_d'$ null on the TS side γ_2^- [4]. This gives

$$\langle[\boldsymbol{n}\times\boldsymbol{e}_2]_{\gamma_2},\boldsymbol{h}'\rangle_{\gamma_2}=\langle[\boldsymbol{n}\times\boldsymbol{e}_2]_{\gamma_2},\boldsymbol{h}_c'\rangle_{\gamma_2}+\langle\boldsymbol{n}\times\boldsymbol{e}_2,\boldsymbol{h}_d'\rangle_{\gamma_2^+}. \quad (24)$$

The $\boldsymbol{e}_p$ trace discontinuity $\langle[\boldsymbol{n}\times\boldsymbol{e}_2]_{\gamma_2},\boldsymbol{h}_c'\rangle_{\gamma_2}$ in (24) is given by (10), i.e.

$$\begin{aligned}\langle[\boldsymbol{n}\times\boldsymbol{e}_2]_{\gamma_2},\boldsymbol{h}_c'\rangle_{\gamma_2} &= \langle[\boldsymbol{n}\times\boldsymbol{e}]_{\gamma_2},\boldsymbol{h}_c'\rangle_{\gamma_2}\\ &= \langle\sigma\beta\partial_t(2\boldsymbol{h}_c+\boldsymbol{h}_d),\boldsymbol{h}_c'\rangle_{\gamma_2}. \end{aligned} \quad (25)$$

The term $\langle\boldsymbol{n}\times\boldsymbol{e}_2,\boldsymbol{h}_d'\rangle_{\gamma_2^+}$ in (24) is given by (11), suppressing $\boldsymbol{n}\times\boldsymbol{e}_1|_{\gamma_2^+}$ of SP 1 and adding the actual TS BC. Thus, the term $\langle\boldsymbol{n}\times\boldsymbol{e}_1,\boldsymbol{h}_d'\rangle_{\gamma_2^+}$ is a SS that can be naturally expressed via the weak formulation of SP 1 in (21), i.e.

$$-\langle\boldsymbol{n}\times\boldsymbol{e}_1,\boldsymbol{h}_d'\rangle_{\gamma_2^+}=(\mu_1\partial_t\boldsymbol{h}_{s1},\boldsymbol{h}_d')_{\Omega_1}+(\mu_1\partial_t\boldsymbol{h}_1,\boldsymbol{h}_d')_{\Omega_1}. \quad (26)$$

The contributions of the volume integrals in (26) are also limited to a single layer of FEs on the positive side of $\Omega_1^+ = \Omega_2^+$ touching $\gamma_2^+ = \gamma_1^+$, because they involve only the trace $\boldsymbol{n}\times\boldsymbol{h}_d'|_{\gamma_2^+}$. At the discrete level, the source $\boldsymbol{h}_1$, initially in mesh of SP 1, has to be projected in mesh of SP 2 [1], [10]. The inaccurate TS SP 2 solution of (22) is then corrected by SP3 via VSs by (12b) and (13b). The weak form for SP 3 is

$$\begin{aligned}&\partial_t(\mu_3\boldsymbol{h}_3,\boldsymbol{h}_3')_{\Omega_3}+(\sigma_3^{-1}\mathrm{curl}\,\boldsymbol{h}_3,\mathrm{curl}\,\boldsymbol{h}_3')_{\Omega_3}+\partial_t(\boldsymbol{b}_{s,3},\boldsymbol{h}_3')_{\Omega_3}\\ &+(\boldsymbol{e}_{s,3},\mathrm{curl}\,\boldsymbol{h}_3')_{\Omega_3}+\langle\boldsymbol{n}\times\boldsymbol{e}_3,\boldsymbol{h}_3'\rangle_{\Gamma_{e3}}=0,\ \forall\boldsymbol{h}_3'\in F_3^1(\Omega_3). \end{aligned} \quad (27)$$

C. TS Correction-VSs in the Actual Volumic Shell

Changes of material properties from μ_2 and σ_2 to μ_3 and σ_3 are taken into account in (20) and (27) via the volume integrals $(\boldsymbol{h}_{s,3},\mathrm{curl}\boldsymbol{a}_3')_{\Omega_3}$, $(\boldsymbol{j}_{s,3},\boldsymbol{a}_3')_{\Omega_3}$ and $(\boldsymbol{e}_{s,3},\mathrm{curl}\boldsymbol{h}_3')_{\Omega_3}$, $\partial_t(\boldsymbol{b}_{s,3},\boldsymbol{h}_3')_{\Omega_3}$, respectively. The VS $\boldsymbol{h}_{s,3}$ is given by (12a), with $\boldsymbol{b}_2 = \mathrm{curl}\boldsymbol{a}_2$ (at the discrete level, the source $\boldsymbol{a}_2$ in (20) is initially given in mesh of SP 2 and must be projected in mesh of SP 3). The VS $\boldsymbol{j}_{s,3}$ is given by (13a), generally reduced to $\boldsymbol{j}_{s,3} = \sigma_3\boldsymbol{e}_2 = \sigma_3(-\partial_t\boldsymbol{a}_2 - \mathrm{grad}v_2)$. Potential v_2 can generally be fixed to zero. The VS $\boldsymbol{e}_{s,3}$ in (13b) is to be obtained from the still undetermined electric field $\boldsymbol{e}_2$, with $\boldsymbol{e}_{s,3} = (\sigma_2/\sigma_3 - 1)\boldsymbol{e}_2$. Indeed, the field $\boldsymbol{e}_2$ is unknown in $\Omega_{c,2}^C$. Its determination requires to solve an electric problem defined by the Faraday and electric conservation equations, with regard to the electric constitutive relation [7].

IV. Application Example

The first test problem is a shielded induction heater. It comprises two stranded inductors, a plate in the middle, and two screens ($\mu_{screen} = 1$, $\sigma_{screen} = 37.7$ MS/m) (2-D, Fig. 1). It is first considered via a SP 1 with the stranded inductors alone (Fig. 2, *top left*, $\boldsymbol{a}_1$), then adding a TS FE SP 2 (Fig. 2, *top right*, $\boldsymbol{a}_2$) that does not include the stranded inductors anymore. Finally, a SP 3 replaces the TS FEs with actual volume FEs (Fig. 2, *bottom middle*, $\boldsymbol{a}_3$). The complete solution is shown as well (Fig. 2, *bottom right*, $\boldsymbol{a}_1 + \boldsymbol{a}_2 + \boldsymbol{a}_3$). The magnetic flux density error on TS SP 2 is pointed out through the relative correction (Fig. 3, *top*), for different plate parameters. Errors can reach 85% in the end regions of the plate. Accurate local corrections with SP 3 are checked to be close to the complete volume FE solution (Fig. 3, *bottom*). Relative corrections of the TS longitudinal magnetic flux and eddy current density are shown in Fig. 4 for different plate thicknesses and frequencies. They can reach several tens of percents in the shells, up to 60% near the screen ends (Fig. 4, *top*), with $\delta = 0.92$ mm, or 40% (Fig. 4, *bottom*), with $\delta = 1.59$ mm.

The second test problem is the TEAM problem 21 (model B, coil and plate, Fig. 5). The inacccuracies on the Joule power

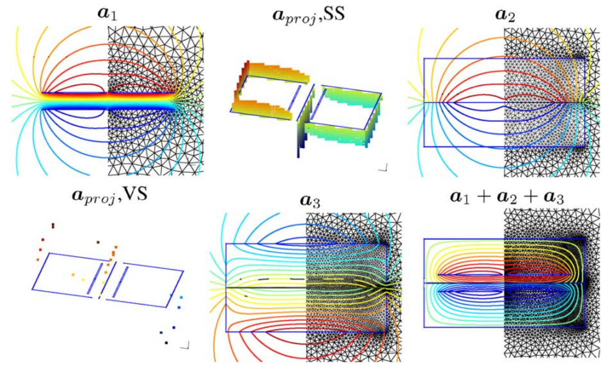

Fig. 2. Flux lines for the SP 1 ($\boldsymbol{a}_1$), SP 2 added ($\boldsymbol{a}_2$), SP 3 solution ($\boldsymbol{a}_3$) and the total solution ($\boldsymbol{a}_1 + \boldsymbol{a}_2 + \boldsymbol{a}_3$) with the different meshes used ($f = 1$ kHz, $\mu_{plate} = 100, \sigma_{plate} = 1$ MS/m). Projection of SP 1 solution ($\boldsymbol{a}_{proj}$, SS) in the SP 2, and of SP 2 solution ($\boldsymbol{a}_{proj}$, VS) in the SP 3.

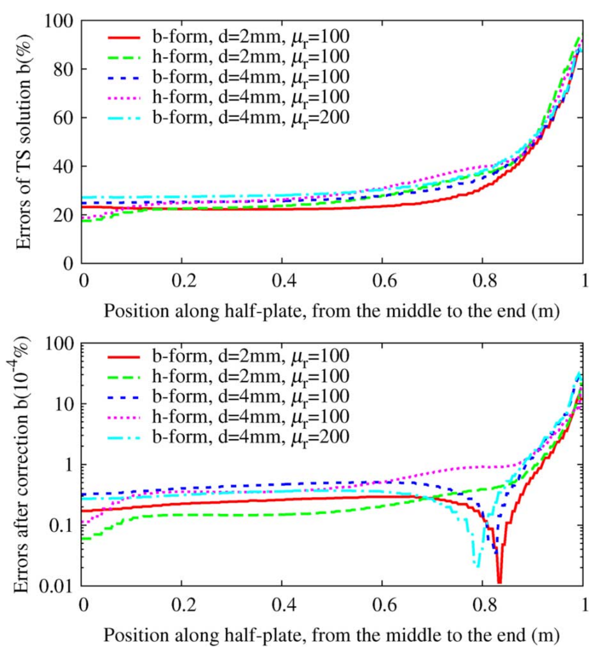

Fig. 3. The TS errors on the magnetic flux density along the plate (*top*) and comparison of the corrected solution (*bottom*) with a classical FE volume model, with different effects of d, μ_r ($\sigma_{plate} = 1$ MS/m, $f = 1$ kHz).

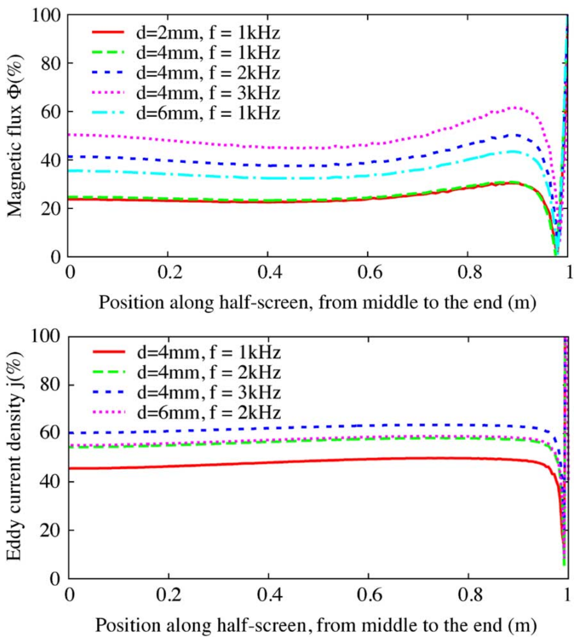

Fig. 4. Relative correction of the longitudinal magnetic flux (*top*) and eddy current density (*bottom*) along the screen for effects of d and frequency f ($\mu_{plate} = 100, \sigma_{plate} = 1$ MS/m), with b-formulation.

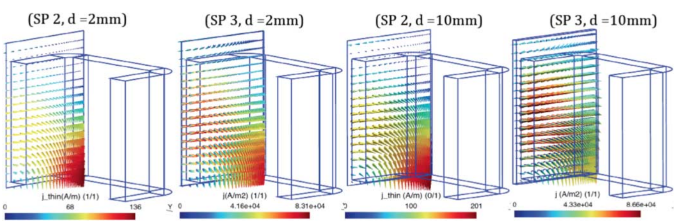

Fig. 5. TEAM problem 21 (1/4th of the geometry, magnetodynamics); eddy current density from TS SP 2 and volume SP 3 respectively, with error reaching 18.85% with $d = 2$ mm (*left pair*) and 77.3% with $d = 10$ mm (*right pair*) ($f = 50$ Hz, $\mu_{plate} = 100, \sigma_{plate} = 6.484$ MS/m).

loss density of TS SP 2 are pointed by the importance of correction SP 3 (Fig. 6). The error on TS SP 2 solution along the vertical half edge (z-direction) can reach 75% at the middle of the plate (Fig. 6, *top*), or 80% along the horizontal half inner width (x-direction) (Fig. 6, *bottom*), with $\delta = 2.975$ mm and $d = 10$ mm in both cases. The errors diminish for a smaller thickness ($d = 2$ mm), being lower than 18.85% (Fig. 6, *top*, *bottom*). Distribution of eddy current density on the TS SP 2 and in the actual volume SP 3 for $d = 2$ mm and $d = 10$ mm are depicted in Fig. 5.

V. Conclusions

The correction of inaccuracies of a TS model has been done via an SPM. Accurate eddy current, power loss density and magnetic flux distributions are successfully obtained at the edges and corners of the thin regions. All the steps of the method have been illustrated and validated with the $\boldsymbol{b}$- and $\boldsymbol{h}$-formulations in 2D and 3D cases. In particular, it has been successfully applied to the TEAM problem 21.

Acknowledgment

This work was supported by the Belgian Sciency Policy (IAP P6/21).

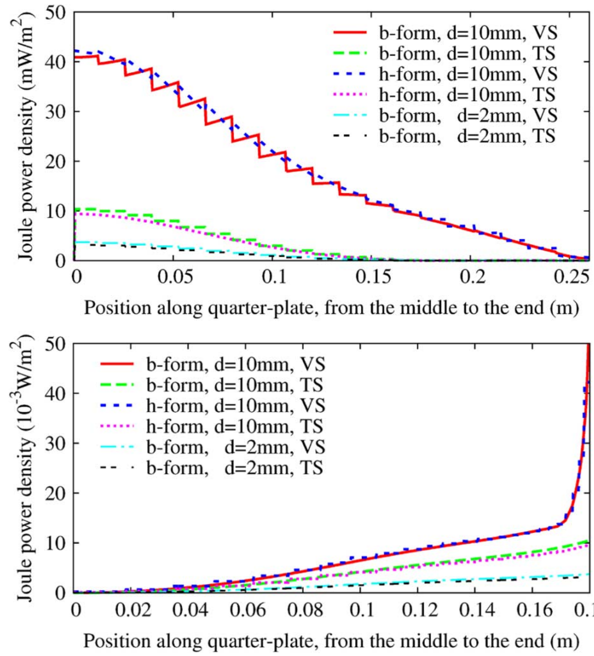

Fig. 6. Joule power loss density between TS and VS solution along vertical half edge (*top*) and horizontal half inner width (*bottom*), with effect of different thicknesses d ($\mu_{plate} = 100, \sigma_{plate} = 6.484$ MS/m and $f = 50$ Hz).

References

[1] P. Dular, V. Q. Dang, R. V. Sabariego, L. Krähenbühl, and C. Geuzaine, "Correction of thin shell finite element magnetic models via a subproblem method," *IEEE Trans. Magn.*, vol. 47, no. 5, pp. 1158–1161, 2011.

[2] P. Dular, R. V. Sabariego, C. Geuzaine, M. V. Ferreira da Luz, P. Kuo-Peng, and L. Krähenbühl, "Finite element magnetic models via a coupling of subproblems of lower dimensions," *IEEE Trans. Magn.*, vol. 46, no. 8, pp. 2827–2830, 2010.

[3] L. Krähenbühl and D. Muller, "Thin layers in electrical engineering. Examples of shell models in analyzing eddy-currents by boundary and finite element methods," *IEEE Trans. Magn.*, vol. 29, no. 2, pp. 1450–1455, 1993.

[4] C. Geuzaine, P. Dular, and W. Legros, "Dual formulations for the modeling of thin electromagnetic shells using edge elements," *IEEE Trans. Magn.*, vol. 36, no. 4, pp. 799–802, 2000.

[5] P. Dular, R. V. Sabariego, M. V. Ferreira da Luz, P. Kuo-Peng, and L. Krähenbühl, "Perturbation finite element method for magnetic model refinement of air gaps and leakage fluxes," *IEEE Trans. Magn.*, vol. 45, no. 3, pp. 1400–1403, 2009.

[6] I. D. Mayergoyz and G. Bedrosian, "On calculation of 3-D eddy currents in conducting and magnetic shells," *IEEE Trans. Magn.*, vol. 31, no. 3, pp. 1319–1324, 1995.

[7] P. Dular and R. V. Sabariego, "A perturbation method for computing field distortions due to conductive regions with h-conform magnetodynamic finite element formulations," *IEEE Trans. Magn.*, vol. 43, no. 4, pp. 1293–1296, 2007.

[8] X. Brunotte and G. Meunier, "Line element for efficent comuptation of the magnetic field created by thin iron plates," *IEEE Trans. Magn.*, vol. 26, no. 3, pp. 2196–2198, 1990.

[9] Z. Ren, "Degenerated Whiney prism elements-general nodal and edge shell elements for field computation in thin structures," *IEEE Trans. Magn.*, vol. 34, no. 05, pp. 2547–2550, 1998.

[10] C. Geuzaine, B. Meys, F. Henrotte, P. Dular, and W. Legros, "A Galerkin projection method for mixed finite elements," *IEEE Trans. Magn.*, vol. 35, no. 3, pp. 1438–1441, 1999.

[11] H. Tsuboi, T. Asahara, F. Kobaysashi, and T. Misaki, "Eddy current analysis on thin conducting plate by an integral equation method using edge elements," *IEEE Trans. Magn.*, vol. 33, no. 2, pp. 1346–1349, 1997.

[12] C. Guerin, G. Tanneau, G. Meunier, X. Brunotte, and J. B. Albertini, "Three dimensional magnetostaic finite elements for gaps and iron shells using magnetic scalar potentials," *IEEE Trans. Magn.*, vol. 30, no. 5, pp. 2885–2888, 1994.